CHAPTER-2

A detailed comparative study on responses of four heat conduction models for an axi-symmetric problem of coupled thermoelastic interactions inside a thick plate

---

2.1 Introduction

Ultrasonic non-destructive testing technique plays an important role for evaluating the quality and lifetime prediction of structures due to its reliability and efficiency. Among the many ways of generating and detecting ultrasonic waves, laser ultrasonic technique has drawn a great attention because of its special non-contact evaluation of materials. However, it has been realized that for the investigation of the wave propagation generated by a laser, we need to consider the thermoelasticity of materials. Furthermore, in aerial and nuclear fields, the thermal effect on wave propagation cannot be ignored because of the extremely high velocity (giving rise to aerodynamic heating) and high temperature. In this chapter, we have considered a problem to analyze the thermoelastic interactions inside an infinitely extended thick plate due to an axi-symmetric temperature distribution applied at the lower and upper surfaces of the plate. We must recall here that an explicit version of the generalized thermoelasiticty theory with two relaxation time parameters was introduced by Green and Lindsay (1972) in which the temperature rates were considered among the constitutive variables. This theory also predicts finite speed of heat propagation as in Lord and Shulman's theory (1967). During 1991-1993, a thermoelasticity theory has been proposed by Green and Naghdi in an alternative way. Their theory was divided into three parts which were subsequently referred to as thermoelastic models of type Green-Naghdi model-I (GN-I), Green-Naghdi model-II (GN-II) and Green-Naghdi model-III (GN-III). Subsequently, the dual phase-lag heat conduction model is proposed by

This work is published in ***International Journal of Thermal Sciences (Elsevier)***, 196-201, 117 (2017).

Tzou (1995) by taking into account the micro structural effects in heat transport process in which one parameter for heat flux vector and other for temperature gradient vector is used.

In this Chapter, we aim to study the present problem in the contexts of the recent heat conduction models, namely Green-Naghdi-I model, Green-Naghdi-II model, dual phase-lag model and Green-Lindsay model. The problem in the contexts of Green-Lindsay model and dual phase-lag model has been studied by Aouadi (2005) and Mukhopadhyay and Kumar (2010), respectively. Therefore, we pay special attention to the thermoelastcity without energy dissipation model given by Green and Naghdi (1993). We investigate the problem under four heat conduction models simultaneously, and we consider the basic governing equations under all these models to formulate our problem in a unified way. The main objective is to compare the results predicted by different models for the present problem and highlight the specific features of the models. We arrange this chapter in the following manner:

In section 2.2, the heat conduction equations under all four models are given which further have been written as a unified way and the governing equations involving the displacement, thermal and stress fields without any heat source or body force in isotropic medium are considered. In section 2.3, the formulation of the problem has been carried out in which homogeneous, isotropic and an infinitely extended thick plate of thickness $2l$ is considered and the Helmholtz decomposition technique is used to decouple the problem. In section 2.4, the boundary conditions have been illustrated in such a way that both the upper and lower planes of the plate have been taken to be traction free and these planes of the plate are subjected to an axi-symmetric temperature distribution. In subsection 2.4.1, Laplace and Hankel transform techniques have been used to solve the problem and the solution has been found out in the transform domain. In subsection 2.4.2, inversion of Hankel transform has been carried out analytically, while in subsection 2.4.3, inversion of Laplace transform has been performed by using short time approximated method. On the basis of the short-time approximated results, discontinuities of physical fields are discussed by using the Boley's theorem (1962) and in subsection 2.4.4, the analytical results have been explained. In section 2.5, the numerical computation is carried out by taking a copper like material and applying a suitable numerical method for Laplace inversion. The numerical solution of the problem is obtained and predictions of all the four models have

been described by graphical presentation of our numerical results. Section 2.6 represents an overall conclusion of the proposed work and investigates the prominent disagreement of the thermoelasticity without energy dissipation model with other models.

2.2 Governing equations

For homogeneous and isotropic elastic medium, the linearized heat conduction equations in the absence of any heat source in the contexts of different models can be written as follows:

Green-Naghdi model-II (GN-II) (1993):

$$K^*\nabla^2 T = (\rho\, c_e \ddot{T} + \gamma T_0 \ddot{e}) \tag{2.1}$$

Green-Naghdi model-I (GN-I) (1991):

$$K\frac{\partial}{\partial t}\nabla^2 T = (\rho\, c_e \ddot{T} + \gamma T_0 \ddot{e}) \tag{2.2}$$

Dual phase-lag model (1995):

$$K(1+\tau_T\frac{\partial}{\partial t})\nabla^2 T = (1+\tau_q\frac{\partial}{\partial t}+\frac{\tau_q^2}{2}\frac{\partial^2}{\partial t^2})(\rho\, c_e \dot{T} + \gamma T_0 \dot{e}) \tag{2.3}$$

Green-Lindsay model (1972):

$$K\nabla^2 T = \rho\, c_e(1+\tau_1\frac{\partial}{\partial t})\dot{T} + \gamma T_0 \dot{e} \tag{2.4}$$

The governing equations involving the displacement, thermal and stress fields without any body force in an isotropic and homogeneous medium can be written as follows:

Equation of motion:

$$\sigma_{ij,\,j} = \rho \ddot{u}_i \tag{2.5}$$

Strain-displacement relation:

$$e_{ij} = \frac{1}{2}(u_{i,j} + u_{j,i}) \tag{2.6}$$

Stress-strain-temperature relation:

$$\sigma_{ij} = \lambda\, e\, \delta_{ij} + 2\mu e_{ij} - \gamma(1+\tau_2\frac{\partial}{\partial t})(T-T_0)\delta_{ij} \tag{2.7}$$

In the above equations, K and K^* are the thermal conductivity and the rate of conductivity, respectively. δ_{ij} is the Kronecker delta symbol. τ_1, τ_2 are thermal relaxation parameters, τ_q and τ_T are the phase-lag parameters. $\tau_2 \neq 0$ for Green-Lindsay model whereas $\tau_2 = 0$ for other three models. T and T_0 are the absolute temperature and reference temperature, respectively. A dot over the variable denotes here the partial derivative with respect to time t. e is the dilatation which can be expressed as

$$e = e_{ii} \tag{2.8}$$

The heat conduction equations given by Eqs. (2.1-2.4) can be re-written after combining in an unified way in the following manner:

$$[K^*\,\delta_{1k} + K\,\delta_{2k}(1+\tau_T\frac{\partial}{\partial t})\frac{\partial}{\partial t}]\nabla^2 T = [\delta_{1k} + \delta_{2k}(1+\tau_q\frac{\partial}{\partial t} + \frac{\tau_q^2}{2}\frac{\partial^2}{\partial t^2})]\frac{\partial}{\partial t}[\rho\, c_e(1+\tau_1\frac{\partial}{\partial t})\dot{T} + \gamma T_0 \dot{e}] \tag{2.9}$$

After putting different values of parameters τ_1, τ_2, τ_q, τ_T, and k in the Kronecker delta functions δ_{1k} and δ_{2k}, we can obtain different heat conduction models as follows:

- **GN-II model:** $k = 1,\ \tau_1 = 0,\ \tau_2 = 0,\ \tau_q = 0,\ \tau_T = 0$
- **GN-I model:** $k = 2,\ \tau_1 = 0,\ \tau_2 = 0,\ \tau_q = 0,\ \tau_T = 0$
- **Dual phase-lag model:** $k = 2,\ \tau_2 = 0,\ \tau_1 = 0,\ \tau_q \neq 0,\ \tau_T \neq 0$
- **Green-Lindsay model:** $k = 2,\ \tau_1 \neq 0,\ \tau_2 \neq 0,\ \tau_q = 0,\ \tau_T = 0$

Therefore, by considering Eqs. (2.5 -2.8) and Eq. (2.9), we can study the present problem under GN-II model, GN-I model, dual phase-lag model and Green-Lindsay model in an unified way. It must be mentioned here that the case under classical coupled thermoelastic model and

Green-Lindsay model have been discussed by Aouadi (2005) and the case under dual-phase-lag model has been reported by Mukhopadhyay and Kumar (2010).

2.3 Formulation of the problem

For the present problem, a homogeneous, isotropic and infinitely extended thick plate of thickness $2l$ is considered which is in undisturbed state and initially at uniform reference temperature T_0. As described in Figures 2.1 (a, b), we assume that $z-$axis is the axis of symmetry and the middle point between the lower and upper surfaces of the plate is taken to be the origin of the cylindrical polar coordinates (r, θ, z). Then the problem for the medium in the region D is defined by:

$$D = \{(r, \theta, z) : 0 \leq r \leq \infty, 0 \leq \theta \leq 2\pi, -l \leq z \leq l\}$$

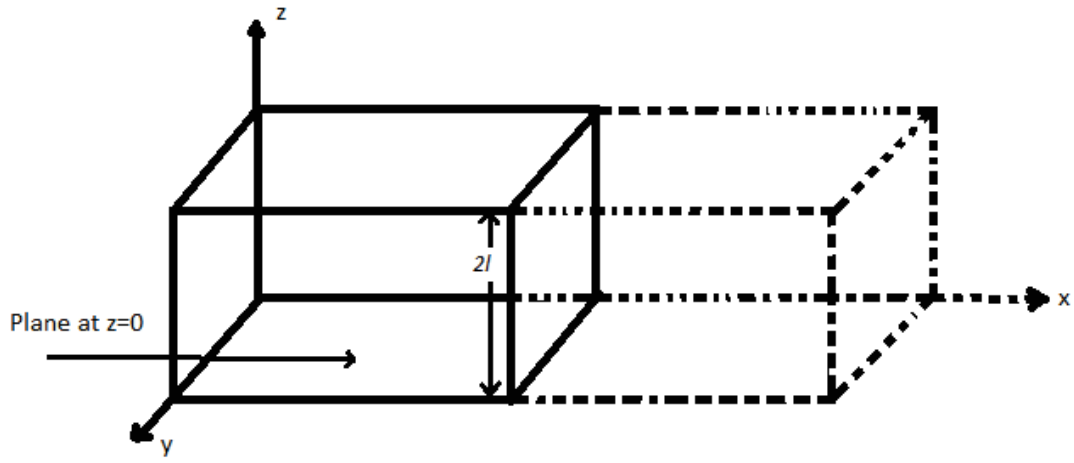

Fig. 2.1(a) An infinitely extended thick plate of thickness $2l$

Therefore, Eq. (5) can be written as

$$\frac{\partial \sigma_{rr}}{\partial r} + \frac{\partial \sigma_{rz}}{\partial z} + \frac{\sigma_{rr} - \sigma_{\theta\theta}}{r} = \rho \frac{\partial^2 u}{\partial t^2} \tag{2.10}$$

$$\frac{\partial \sigma_{rz}}{\partial r} + \frac{\partial \sigma_{zz}}{\partial z} + \frac{\sigma_{rz}}{r} = \rho \frac{\partial^2 w}{\partial t^2} \tag{2.11}$$

where, $u = u(r, z, t)$ and $w = w(r, z, t)$, are the displacement components in the r and z directions, respectively for the present axi-symmetric problem.

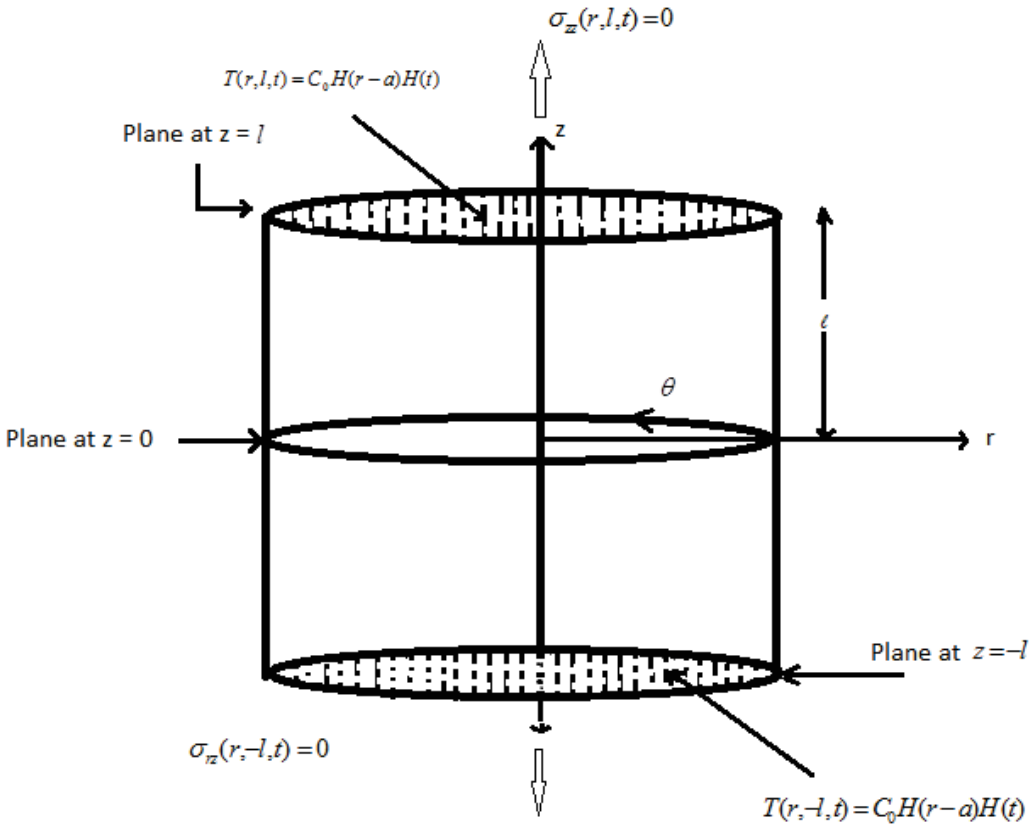

Fig. 2.1(b) Axi-symmetric temperature distribution in the cylindrical co-ordinate with z-axis as the axis of symmetry

Now, the following non-dimensional quantities have been introduced:

$c_1^2=\frac{\lambda+2\mu}{\rho}$, $r'=c_1\eta\, r$, $u'=c_1\eta u$, $t'=c_1^2\eta\, t$, $\tau_1'=c_1^2\eta\,\tau_1$, $\tau_2'=c_1^2\eta\,\tau_2$, $\mu_1=\frac{\mu}{\lambda+2\mu}$, $a_1=\frac{\gamma T_0}{(\lambda+2\mu)}$,

$\tau_q'=c_1^2\eta\,\tau_q$, $\tau_T'=c_1^2\eta\,\tau_T$, $T'=\frac{T-T_0}{T}$, $\sigma_{rr}'=\frac{\sigma_{rr}}{\mu}$, $\sigma_{\theta\theta}'=\frac{\sigma_{\theta\theta}}{\mu}$, $a_2=\frac{\gamma}{K\eta}$, $a_0=\frac{K^*}{Kc_1^2\eta}$, $\lambda_1=\frac{\lambda}{\mu}$, $\beta=\frac{a_1}{\mu_1}$

In what follows, we drop the prime notations from all the quantities for convenience.

In view of the above, the dimensionless stress components derived from Eq. (2.7) are given by

$$\sigma_{rr}=2e_{rr}+\lambda_1 e-\beta(1+\tau_2\frac{\partial}{\partial t})T \tag{2.12}$$

$$\sigma_{\theta\theta}=2e_{\theta\theta}+\lambda_1 e-\beta(1+\tau_2\frac{\partial}{\partial t})T \tag{2.13}$$

$$\sigma_{zz} = 2\,e_{zz} + \lambda_1 e - \beta(1+\tau_2\frac{\partial}{\partial t})\,T \tag{2.14}$$

$$\sigma_{rz} = 2\,e_{rz} \tag{2.15}$$

and non-dimensional strain components can be written as

$$e_{rr} = \frac{\partial u}{\partial r},\ e_{\theta\theta} = \frac{u}{r},\ e_{zz} = \frac{\partial w}{\partial z}, e_{rz} = \frac{1}{2}(\frac{\partial u}{\partial z} + \frac{\partial w}{\partial r})$$

Now, Eqs. (2.9-2.11) can be written in following non-dimensional forms:

$$[a_0\,\delta_{1k} + \delta_{2k}(1+\tau_T\frac{\partial}{\partial t})\frac{\partial}{\partial t}]\nabla^2 T = [\delta_{1k} + \delta_{2k}(1+\tau_q\frac{\partial}{\partial t} + \frac{\tau_q^2}{2}\frac{\partial^2}{\partial t^2})]\frac{\partial}{\partial t}[(1+\tau_1\frac{\partial}{\partial t})\dot{T} + a_2\dot{e}] \tag{2.16}$$

$$\mu_1\nabla^2 u - \mu_1\frac{u}{r^2} + (1-\mu_1)\frac{\partial e}{\partial r} - a_1(1+\tau_2\frac{\partial}{\partial t})\frac{\partial T}{\partial r} = \frac{\partial^2 u}{\partial t^2} \tag{2.17}$$

$$\mu_1\nabla^2 w + (1-\mu_1)\frac{\partial e}{\partial z} - a_1(1+\tau_2\frac{\partial}{\partial t})\frac{\partial T}{\partial z} = \frac{\partial^2 w}{\partial t^2} \tag{2.18}$$

where,

$$\nabla^2 = (\frac{\partial^2}{\partial r^2} + \frac{1}{r}\frac{\partial}{\partial r} + \frac{\partial^2}{\partial z^2})$$

Now, with the help of the Helmholtz decomposition, we can write the displacement components u and w as follows:

$$u = \frac{\partial \phi}{\partial r} + \frac{\partial^2 \psi}{\partial r \partial z} \tag{2.19}$$

$$w = \frac{\partial \phi}{\partial z} - \frac{\partial^2 \psi}{\partial r^2} - \frac{1}{r}\frac{\partial \psi}{\partial r} \tag{2.20}$$

where, ϕ and ψ are the scalar and vector potential functions, representing the dilatation and rotational part of the displacement vector. We also obtain

$$e = \nabla^2 \phi \tag{2.21}$$

From the Eqs. (2.19-2.21) and (2.16-2.18), we obtain a system of equations containing the displacement potentials ϕ, ψ along with the temperature field T as follows:

$$[\{a_0\,\delta_{1k} + \delta_{2k}(1+\tau_T\frac{\partial}{\partial t})\frac{\partial}{\partial t}\}\nabla^2 - \{\delta_{1k} + \delta_{2k}(1+\tau_q\frac{\partial}{\partial t} + \frac{\tau_q^2}{2}\frac{\partial^2}{\partial t^2})\}\frac{\partial}{\partial t}(1+\tau_1\frac{\partial}{\partial t})\frac{\partial}{\partial t}]T$$

$$= a_2\{\delta_{1k} + \delta_{2k}(1+\tau_q\frac{\partial}{\partial t} + \frac{\tau_q^2}{2}\frac{\partial^2}{\partial t^2})\}\frac{\partial^2}{\partial t^2}\nabla^2\phi \tag{2.22}$$

$$\nabla^2\phi - \frac{\partial^2\phi}{\partial t^2} = a_1(1+\tau_2\frac{\partial}{\partial t})T \tag{2.23}$$

$$\nabla^2\psi - \frac{1}{\mu_1}\frac{\partial^2\psi}{\partial t^2} = 0 \tag{2.24}$$

From Eqs. (2.22-2.24), it is clear that ϕ and T are coupled together, whereas ψ is not coupled with ϕ and T. This implies that Eq. (2.24) indicates the shear motion which is not affected by the thermal field and it is purely elastic in nature. However, Eqs. (2.22-2.23) represent the field functions ϕ and T included in the coupled thermoelastic motion.

2.3.1 Boundary Conditions

From the assumptions of the problem and the geometry given in Figure 2.1 (b), it is clear that both the upper and lower planes of the plate are traction free which implies that the mechanical boundary conditions are taken to be stress free which means

$$\sigma_{zz}(r,\pm l,t) = 0, \;\; \sigma_{rz}(r,\pm l,t) = 0 \tag{2.25}$$

and both the upper and lower boundary planes of the plate are subjected to an axi-symmetric temperature distribution and given as

$$T(r, \pm l, t) = C_0 H(a-r) H(t) \tag{2.26}$$

where, $H(.)$ is the Heaviside unit step function and it is considered that the temperatures of the lower and upper boundaries suddenly increase at $t = 0$ such that the temperature of a circular region $r \leq a$ of both the upper and lower boundaries obtain a fixed value C_0.

2.4 Solution of the problem

2.4.1 Laplace and Hankel transforms

Now, the Laplace transform of a function $f(r, t)$ can be defined in the form

$$\bar{f}(r, p) = \int_0^\infty e^{-pt} f(r, t)\, dt$$

whereas the Hankel transform of a function $f(r, t)$ can be defined as

$$f^*(\alpha, t) = \hbar(f(r, t)) = \int_0^\infty r\, f(r, t)\, J_0(\alpha r)\, dr$$

where, p and α are representing the Laplace and Hankel transform parameters, respectively and $J_0(.)$ is the Bessel function of first kind of order zero. $\bar{f}(r, p)$ and $f^*(\alpha, t)$ are the Laplace and Hankel transform of $f(r, t)$ with respect to r and t, respectively, whereas $\bar{f}^*(\alpha, p)$ denotes the Hankel transform of $\bar{f}(r, p)$.

By considering the homogeneous initial conditions and applying the Laplace transform and then Hankel transforms to Eqs. (2.22-2.24), we find

$$[\{a_0\, \delta_{1k} + \delta_{2k}(1 + \tau_T\, p)p\}(\frac{\partial^2}{\partial z^2} - \alpha^2) - \{\delta_{1k} + \delta_{2k}(1 + \tau_q\, p + \frac{\tau_q^2}{2} p^2)\} p(1 + \tau_1\, p)p]\bar{T}^*$$

$$= a_2\{\delta_{1k} + \delta_{2k}(1 + \tau_q\, p + \frac{\tau_q^2}{2}\, p^2)\} p^2 (\frac{\partial^2}{\partial z^2} - \alpha^2)\bar{\phi}^* \tag{2.27}$$

$$(\frac{\partial^2}{\partial z^2} - \alpha^2 - p^2)\bar{\phi}^* = a_1(1+\tau_2 p)\bar{T}^* \tag{2.28}$$

$$(\frac{\partial^2}{\partial z^2} - \alpha^2 - \frac{1}{\mu_1}p^2)\bar{\psi}^* = 0 \tag{2.29}$$

Now, with the elimination of $\bar{T}^*$ from Eqs. (2.27-2.28), we obtain the equation having $\bar{\phi}^*$ in the terms as given below

$$(\frac{\partial^2}{\partial z^2} - m_1^2)(\frac{\partial^2}{\partial z^2} - m_2^2)\bar{\phi}^* = 0 \tag{2.30}$$

where, $\pm m_1$ and $\pm m_2$ are the roots of the following equation:

$$A(p)m^4 - \{2A(p)\alpha^2 + A(p)p^2 + B_1(p) + \varepsilon B_2(p)\}m^2 + \{\alpha^2(\alpha^2+p^2)A(p) + (p^2+\alpha^2)B_1(p) + \varepsilon\alpha^2 B_2(p)\} = 0 \tag{2.31}$$

where, $A(p) = [a_0\delta_{1k} + \delta_{2k}(1+\tau_T p)p]$, $B(p) = [\delta_{1k} + \delta_{2k}(1+\tau_q p + \frac{\tau_q^2}{2}p^2)]p^2$, $B_1(p) = B(p)(1+\tau_1 p)$, $B_2(p) = B(p)(1+\tau_2 p)$, $\varepsilon = a_1 a_2 = \frac{\gamma^2 T_0}{\rho^2 c_v c_1^2}$ and $\rho c_v = K\eta$.

where, ε denotes the thermoelastic coupling constant.

In present work, the problem has been treated as axi-symmetric problem in which z-axis is the axis of symmetry. Here, w is the displacement component along $z-$direction and u is the displacement component along r-direction. Hence, it is clear that due to symmetry of the problem, u is the even function of z and w is the odd function of z. Further, we also assumed that temperature distribution is axi-symmetric about z- axis. Therefore, T is also evidently an even function of z.

Therefore, from Eqs. (2.19-2.20), we conclude that ϕ and ψ are also the even and odd functions of z, respectively. Hence, the expressions for $\bar{\phi}^*$, $\bar{\psi}^*$ and $\bar{T}^*$ are finally obtained as

$$\bar{\phi}^* = \sum_{i=1}^{2} A_i \, cosh(m_i z) \tag{2.32}$$

$$\bar{\psi}^* = C \, sinh(q z) \tag{2.33}$$

$$a_1(1+\tau_2 p)\bar{T}^* = \sum_{i=1}^{2}(m_i^2-\alpha^2-p^2)\,A_i\,cosh(m_i z) \tag{2.34}$$

where, $q^2 = \alpha^2 + \frac{1}{\mu_1}p^2$.

In Eqs. $(2.32-2.34)$, A_1, A_2 and C are arbitrary constants which are the functions of both p and α but they are independent of z.

From Eqs. (2.14), (2.15), (2.19), (2.20) and (2.32-2.34), we find the stresses $\bar{\sigma}_{zz}^*$ and $\bar{\sigma}_{rz}^*$ in the terms given as

$$\bar{\sigma}_{zz}^* = (\frac{1}{\mu_1}p^2+2\alpha^2)\bar{\phi}^* + 2\alpha^2\frac{\partial\bar{\psi}^*}{\partial z} \tag{2.35}$$

$$\bar{\sigma}_{rz}^* = \hbar(\frac{\partial}{\partial r}(2\frac{\partial\bar{\phi}}{\partial z}+(2\frac{\partial^2}{\partial z^2}-\frac{p^2}{\mu_1})\bar{\psi})) \tag{2.36}$$

By using the boundary conditions given by Eqs. (2.25) and (2.26) along with Eqs. (2.32-2.36), we obtain

$$\sum_{i=1}^{2}(\frac{1}{\mu_1}p^2+2\alpha^2)A_i\,cosh(m_i l) = -2\alpha^2 qC\,cosh(ql) \tag{2.37}$$

$$\sum_{i=1}^{2} m_i A_i\,sinh(m_i l) = \frac{1}{2}(\frac{p^2}{\mu_1}-2q^2)C\,sinh(ql) \tag{2.38}$$

$$\sum_{i=1}^{2}(m_i^2-\alpha^2-p^2)A_i\,cosh(m_i l) = \frac{aa_1(1+\tau_2 p)C_0}{\alpha p}J_1(\alpha a) \tag{2.39}$$

Thus, we obtain the constants A_1, A_2 and C from Eqs. (2.37-2.39) in the forms as

$A_1 = -\frac{a_1(1+\tau_2 p)(4\alpha^2 q m_2\mu_1^2 tanh(m_2 l)-(2\alpha^2\mu_1+p^2)^2 tanh(ql))}{pX\,cosh(m_1 l)(2\alpha^2\mu_1+p^2)^2 tanh(ql)}\theta_0^*(\alpha)$,

$A_2 = \frac{a_1(1+\tau_2 p)(4\alpha^2 q m_1\mu_1^2 tanh(m_1 l)-(2\alpha^2\mu_1+p^2)^2 tanh(ql))}{pX\,cosh(m_2 l)(2\alpha^2\mu_1+p^2)^2 tanh(ql)}\theta_0^*(\alpha)$,

$C = \frac{2a_1(1+\tau_2 p)\mu_1[m_2 tanh(m_2 l)-m_1 tanh(m_1 l)]}{pX(2\alpha^2\mu_1+p^2)sinh(ql)}\theta_0^*(\alpha)$,

where, $\theta_0^*(\alpha) = \frac{aC_0}{\alpha}J_1(\alpha a)$ and

$X = m_1^2 - m_2^2 + \frac{4\alpha^2 q\mu_1^2}{(2\alpha^2\mu_1+p^2)^2 tanh(ql)}[m_1(m_2^2-\alpha^2-p^2)tanh(m_1 l) - m_2(m_1^2-\alpha^2-p^2)tanh(m_2 l)]$

Therefore, the solution has been obtained in the transformed domain.

2.4.2 Inversion of the Hankel transform

Now, the inverse of Hankel transform of $\bar{f}^*(\alpha, p)$ can be defined in the following manner:

$$\bar{f}(r, p) = \hbar^{-1}[\bar{f}^*(\alpha, p)] = \int_0^\infty \bar{f}^*(\alpha, p)\alpha J_0(\alpha r)\, d\alpha \tag{2.40}$$

Hence, by using the inverse Hankel transform to Eqs. (2.32-2.34), we obtain

$$a_1(1+\tau_2 p)\bar{T}(r, z, p) = \int_0^\infty \alpha J_0(\alpha r) \sum_{i=1}^{2} A_i(m_i^2 - \alpha^2 - p^2)\, cosh(m_i z)\, d\alpha \tag{2.41}$$

$$\bar{\phi}(r, z, p) = \int_0^\infty \alpha J_0(\alpha r) \sum_{i=1}^{2} A_i\, cosh(m_i z)\, d\alpha \tag{2.42}$$

$$\bar{\psi}(r, z, p) = \int_0^\infty \alpha J_0(\alpha r)\, C\, sinh(qz) \tag{2.43}$$

Further, by putting Eqs. (2.41-2.43) into the Eqs. (2.17-2.20), we get the solutions for the displacement components in the Laplace transform domain in the forms given as

$$\bar{u}(r, z, p) = -\int_0^\infty \alpha^2 J_1(\alpha r)\,[\sum_{i=0}^{2} A_i\, cosh(m_i z) + C\, q\, cosh(qz)]\, d\alpha \tag{2.44}$$

$$\bar{w}(r, z, p) = \int_0^\infty \alpha J_0(\alpha r)\,[\sum_{i=1}^{2} m_i A_i\, sinh(m_i z) + C\,\alpha^2\, sinh(qz)]\, d\alpha \tag{2.45}$$

Now, using the Laplace transform to both sides of Eqs. (2.12-2.14) and with the help of the solutions given by Eqs. (2.41-2.45), the stress components are found in the Laplace transform domain as

$$\begin{aligned}\bar{\sigma}_{rr} = {} & \textstyle\int_0^\infty \sum_{i=1}^{2} \{\frac{2\alpha^2}{r} J_1(\alpha r) + \alpha J_0(\alpha r)\,(\frac{p^2}{\mu_1} - 2m_i^2)\}\, A_i\, cosh(m_i z)\, d\alpha \\ & + \textstyle\int_0^\infty 2\alpha^3 [\frac{1}{\alpha r} J_1(\alpha r) - J_0(\alpha r)]\, C\, q\, cosh(qz)\, d\alpha\end{aligned} \tag{2.46}$$

$$\begin{aligned}\bar{\sigma}_{\theta\theta} = {} & \textstyle\int_0^\infty \sum_{i=1}^{2} [\alpha J_0(\alpha r)\,(\frac{p^2}{\mu_1} + 2\alpha^2 - 2m_i^2) - \frac{2}{r}\alpha^2 J_1(\alpha r)]\, A_i\, cosh(m_i z)\, d\alpha \\ & - \tfrac{2}{r} \textstyle\int C q\, \alpha^2 J_1(\alpha r)\, cosh(qz)\, d\alpha\end{aligned} \tag{2.47}$$

$$\begin{aligned}\bar{\sigma}_{zz} = \int_0^\infty \alpha J_0(\alpha r)\{(\tfrac{p^2}{\mu_1}+2\alpha^2)[\textstyle\sum_{i=1}^{2} A_i \cosh(m_i z)] \\ +2\alpha^2 qC\cosh(qz)\}\, d\alpha\end{aligned} \tag{2.48}$$

The Eqs. (2.41-2.48) are the solutions of physical field variables in Laplace transform domain.

2.4.3 Inversion of the Laplace transform

2.4.3.1 Short-time approximated solutions and discussions

In view of the solutions of different field variables in Laplace transform domain obtained in the previous section, we note that the Eqs. (2.41-2.48) are having the complicated terms containing the Laplace transform parameter, p which is very critical to invert them and get closed form analytical solutions in physical domain. Hence, we attempt to apply the short-time approximation technique to invert the Laplace transform which is applicable only for large values of Laplace parameter, p and thereafter, we use the Boley's theorem (1962) to find out the locations of the physical field variables where they have discontinuities. In addition to finding out the locations of wave fronts, this theorem is also very useful to find the exact values of speeds directly from the Laplace transform expressions without actually inverting these expressions when the field variables are having the exponential term.

To use this Boley's theorem, we proceed as follows: First of all, we consider p to be very large and expand all the terms contained in Eq. (2.31) in power of $\frac{1}{p}$ to find out the roots of the Eq. (2.31) by neglecting the higher powers for smallness due to large value of p. The problem under dual-phase lag model has been discussed by Mukhopadhyay and Kumar (2010). Hence, We skip to find the short-time approximated solutions under dual phase-lag model, although our main objective is to observe the behavior of physical field variables under GN-II model and compare them with the same for other models.

The roots of Eq. (2.31) under GN-I model, GN-II model and Green-Lindsay model have been found out as follows:

GN-II model:

$$m_1 = pM_1 + M_2\frac{1}{p} + O(\frac{1}{p^2}) \tag{2.49}$$

$$m_2 = pN_1 + N_2\frac{1}{p} + O(\frac{1}{p^2}) \tag{2.50}$$

GN-I model:

$$m_1 = p + M_{11} + M_{12}\frac{1}{p} + O(\frac{1}{p^2}) \tag{2.51}$$

$$m_2 = \sqrt{p} + N_{11}\frac{1}{\sqrt{p}} + O(\frac{1}{p}) \tag{2.52}$$

Green-Lindsay model:

$$m_1 = \sqrt{A_1}p + M_{31} + M_{32}\frac{1}{p} + O(\frac{1}{p^2}) \tag{2.53}$$

$$m_2 = \sqrt{A_1'}p + N_{31} + N_{32}\frac{1}{p} + O(\frac{1}{p^2}) \tag{2.54}$$

where, the different notations used above have been defined as

$M_1 = \sqrt{\frac{a_0+\varepsilon_1}{a_0} - \frac{1}{a_0+\varepsilon_1}}, M_2 = \frac{\alpha^2}{2M_1}, N_1 = \sqrt{\frac{1}{a_0+\varepsilon_1}}, N_2 = \frac{\alpha^2}{2N_1}, M_{11} = \frac{\varepsilon}{2}, M_{12} = (\frac{\alpha^2\varepsilon}{2} - \frac{\varepsilon^2}{8}), N_{11} = \frac{\alpha^2-\varepsilon}{2}$,

$M_{31} = \frac{A_2}{2\sqrt{A_1}}, M_{32} = \frac{A_3}{2\sqrt{A_1}}, N_{31} = \frac{A_2'}{2\sqrt{A_1'}}, N_{32} = \frac{A_3'}{2\sqrt{A_1'}}, A_1 = \frac{1}{2}[(1+\tau_1+\varepsilon\tau_2) + \sqrt{A'}], A_2 = \frac{1}{2}(\varepsilon_1 + \frac{B'}{2\sqrt{A'}})$,

$A_3 = \frac{1}{2}(2\alpha^2 + \frac{\varepsilon_1^2}{\sqrt{A'}})$, $A_1' = \frac{1}{2}[(1+\tau_1+\varepsilon\tau_2) - \sqrt{A'}], A_2' = \frac{1}{2}(\varepsilon_1 - \frac{B'}{2\sqrt{A'}}), A_3' = \frac{1}{2}(2\alpha^2 - \frac{\varepsilon_1^2}{\sqrt{A'}})$,

$A' = [(1+\tau_1+\varepsilon\tau_2)^2 - 4\tau_1], B' = [2\varepsilon_1(1+\tau_1+\varepsilon\tau_2) - 4\tau_1]$, $\varepsilon_1 = 1+\varepsilon$,

Further, for p, to be very large

$tanh(m_i l) = tanh(ql) = 1 + O(\frac{1}{p})$, $cosh(m_i l) = \frac{1}{2}e^{m_i l} + O(\frac{1}{p})$, $sinh(ql) = \frac{1}{2}e^{ql} + O(\frac{1}{p})$

Now, we obtain the approximated solutions for temperature field variables in the Laplace parameter domain under three models after putting the above expressions of m_1 and m_2 from Eqs. (2.49-2.54) into Eq. (2.41), as follows:

GN-II model:

$$\bar{T}(r,z,p) = [\frac{(M_1^2-1)}{(M_1^2-N_1^2)}\frac{1}{p}\int_0^\infty \alpha J_0(\alpha r)\,\theta_0^*(\alpha)\,e^{m_1(z-l)}d\alpha + \frac{(M_1^2-1)}{(M_1^2-N_1^2)}\frac{1}{p}\int_0^\infty \alpha J_0(\alpha r)\,\theta_0^*(\alpha)\,e^{-m_1(z+l)}d\alpha$$
$$+\frac{(N_1^2-1)}{(N_1^2-M_1^2)}\frac{1}{p}\int_0^\infty \alpha J_0(\alpha r)\,\theta_0^*(\alpha)\,e^{m_2(z-l)}d\alpha + \frac{(N_1^2-1)}{(N_1^2-M_1^2)}\frac{1}{p}\int_0^\infty \alpha J_0(\alpha r)\,\theta_0^*(\alpha)\,e^{-m_2(z+l)}d\alpha] + O(\frac{1}{p^2}) \tag{2.55}$$

GN-I model:

$$\bar{T}(r,z,p) = [\frac{2M_{11}}{p^2}\int_0^\infty \alpha J_0(\alpha r)\,\theta_0^*(\alpha)\,e^{m_1(z-l)}d\alpha + \frac{2M_{11}}{p^2}\int_0^\infty \alpha J_0(\alpha r)\,\theta_0^*(\alpha)\,e^{-m_1(z+l)}d\alpha] + O(\frac{1}{p^3})$$
$$+[\frac{1}{p}\int_0^\infty \alpha J_0(\alpha r)\,\theta_0^*(\alpha)\,e^{m_2(z-l)}d\alpha + \frac{1}{p}\int_0^\infty \alpha J_0(\alpha r)\,\theta_0^*(\alpha)\,e^{-m_2(z+l)}d\alpha] + O(\frac{1}{p^2}) \tag{2.56}$$

Green-Lindsay model:

$$\bar{T}(r,z,p) = [\tfrac{A_1-1}{A_1-A_1'}\tfrac{1}{p}\int_0^\infty \alpha J_0(\alpha r)\,\theta_0^*(\alpha)\,e^{m_1(z-l)}d\alpha + \tfrac{A_1-1}{A_1-A_1'}\tfrac{1}{p}\int_0^\infty \alpha J_0(\alpha r)\,\theta_0^*(\alpha)\,e^{-m_1(z+l)}d\alpha$$
$$+\tfrac{A_1'-1}{A_1'-A_1}\tfrac{1}{p}\int_0^\infty \alpha J_0(\alpha r)\,\theta_0^*(\alpha)\,e^{m_2(z-l)}d\alpha + \tfrac{A_1'-1}{A_1'-A_1}\tfrac{1}{p}\int_0^\infty \alpha J_0(\alpha r)\,\theta_0^*(\alpha)\,e^{-m_2(z+l)}d\alpha] + O(\tfrac{1}{p^2}) \tag{2.57}$$

Next, we apply Boely's theorem (1962) to identify the nature of discontinuities of the physical field variables, in the following manner:

Using Boely's theorem (see Appendix-A1) into Eqs. (2.55-2.57), we can obtain the following information:

The inverse Laplace transform of the first term in Eq. (2.55) can be written as

$$I_1 = \frac{1}{2\pi i}\int_{d-i\infty}^{d+i\infty} \frac{(M_1^2-1)}{(M_1^2-N_1^2)}\frac{1}{p}\int_0^\infty \alpha J_0(\alpha r)\,\theta_0^*(\alpha)\,e^{m_1(z-l)+pt}d\alpha\,dp$$

The above equation can be re-written as

$$I_1 = \frac{1}{2\pi i}\int_{d-i\infty}^{d+i\infty} \frac{K'}{p}[1+O(\frac{1}{p})]\,e^{f(p,t)}dp \tag{2.58}$$

where, $K' = \frac{(M_1^2-1)}{(M_1^2-N_1^2)}\int_0^\infty \alpha J_0(\alpha r)\,\theta_0^*(\alpha)\,d\alpha$, and $f(p,t) = m_1(z-l)+pt$

and with the help of Eq. (2.49), we find $f(p,t) - p\,\eta(t) = O(\frac{1}{p})$, where $\eta(t) = M_1(z-l)+t$

Similarly, we can invert the remaining terms which are in Eq. (2.55).

The inverse Laplace transform of the first term in Eq. (2.56) can be written as

$$I_2 = \frac{1}{2\pi i}\int_{d-i\infty}^{d+i\infty} \frac{2M_{11}}{p^2}\int_0^{\infty} \alpha J_0(\alpha r)\,\theta_0^*(\alpha)\,e^{m_1(z-l)+pt}d\alpha\,dp$$

This can be re-written as

$$I_2 = \frac{1}{2\pi i}\int_{d-i\infty}^{d+i\infty} \frac{K'}{p^2}[1+O(\frac{1}{p})]\,e^{f(p,t)}dp \tag{2.59}$$

where $K' = 2M_{11}\,e^{-\frac{\varepsilon}{2}(z-l)}\int_0^{\infty}\alpha J_0(\alpha r)\,\theta_0^*(\alpha)\,d\alpha$, and $f(p,t) = m_1(z-l)+pt$.

Hence, with the help of Eq. (2.51), we find $f(p,t) - p\,\eta(t) = O(\frac{1}{p})$, where, $\eta(t) = (z-l)+t$.

Similarly, we can invert the remaining terms which are in Eq. (2.56).

The inverse Laplace transform of the first term in Eq. (2.57) can be written as

$$I_3 = \frac{1}{2\pi i}\int_{d-i\infty}^{d+i\infty} (\frac{A_1-1}{A_1-A_1'})\frac{1}{p}\int_0^{\infty} \alpha J_0(\alpha r)\,\theta_0^*(\alpha)\,e^{m_1(z-l)+pt}d\alpha\,dp$$

which can be re-written as

$$I_3 = \frac{1}{2\pi i}\int_{d-i\infty}^{d+i\infty} \frac{K'}{p}[1+O(\frac{1}{p})]\,e^{f(p,t)}dp \tag{2.60}$$

where, $K' = (\frac{A_1-1}{A_1-A_1'})\,e^{-\frac{A_2}{2\sqrt{A_1}}(z-l)}\int_0^{\infty}\alpha J_0(\alpha r)\,\theta_0^*(\alpha)\,d\alpha$, and $f(p,t) = m_1(z-l)+pt$.

Hence, with the help of Eq. (2.53), we find $f(p,t) - p\,\eta(t) = O(\frac{1}{p})$, where, $\eta(t) = \sqrt{A_1}(z-l)+t$.

Similarly, we can invert the remaining terms which are in Eq. (2.57). In similar way, we obtain the short-time approximated results in the physical domain for other field variables.

2.4.4 Discussion on analytical results

In this section, we aim to analyze the results which are obtained in the previous section. The inversion of Laplace transforms given by Eqs. (2.55-2.57) can be obtained in the forms which are given by Eqs. (2.58-2.60). We firstly observe here that for all three models, the first two terms

of Eqs. (2.55-2.57) which are the solution of temperature fields for the models: GN-II model, GN-I model, Green-Lindsay model, represent the waves originating at the upper surface $(z = l)$ and lower surface $(z = -l)$ of the plate, respectively. From Eqs. (2.49-2.54), the expressions for M_1 and A_1 are indicating that the elastic waves propagate with the finite speeds, $v_e = 1/M_1$ and $v_e = 1/\sqrt{A_1}$, respectively for GN-II model and Green-Lindsay model, while in the case of GN-I model, elastic wave is moving with finite speed unity. These waves are modified elastic waves which reach at the middle plane of plate at time $M_1 l$ and $\sqrt{A_1} l$ under GN-II model and Green-Lindsay model, respectively. However, in the case of GN-I model, this time is l. The third and fourth terms in Eqs. (2.55-2.57) are the waves originating at the upper $(z = l)$ and lower $(z = -l)$ surface of the plate. These waves correspond to the modified thermal waves propagating with speeds $v_t = 1/N_1$ and $v_t = 1/\sqrt{A_1'}$ in the case of GN-II model and Green-Lindsay model, respectively and they arrive the middle plane of the plate at time $N_1 l$ and $\sqrt{A_1'} l$ under GN-II model and Green-Lindsay model, respectively. However, under GN-I model, these terms are diffusive in nature due to presence of damping term in heat conduction equation. From above, we find that all the results under Green-Lindsay model are found to be exactly similar in nature with the corresponding solutions reported by Aouadi (2005) with some changes of notations. We also note that, in the context of dual phase lag model, as reported by Mukhopadhyay and Kumar (2010), the solution of temperature field consists of four terms. Out of these, the first and second terms show the waves originating at the upper and lower surface of the plate which are modified elastic waves and these waves also propagate with finite speeds and reach the middle plane of the plate at the approximate finite non dimensional time. The third and fourth terms represent the waves originating at the lower and upper surface of the plate which are the modified thermal waves and these waves also move with the finite speed. From Eqs. (2.49-2.54), it is clear that M_1 depends on the thermoelastic coupling constant ε as well as K^* that is the material parameter characteristic to the theory of Green and Naghdi of type-II. Further, in case of Green-Lindsay model, the finite speed of wave depends on the thermoelastic coupling constant ε as well as on two thermal relaxation parameters τ_1 and τ_2 that are the characteristic to the theory of Green and Lindsay.

The solutions as given by Eqs. (2.49-2.54) and Eqs. (2.55-2.57) predict that both the elastic

and thermal waves move without any attenuation under GN-II model, while in the case of Green-Lindsay model, these waves are moving with attenuation which is decaying exponentially. This is similar to the case as reported by Aouadi (2005). However, in the case of GN-I model, we find that only the modified elastic waves are moving with finite attenuation $\frac{\varepsilon}{2}$. These waves are observed to propagate with exponentially decaying attenuation in the case of dual phase lag model which has been reported by Mukhopadhyay and Kumar (2010). Difference in the nature of waves under different models can be observed in details from table 2.1(a).

	Elastic wave		Thermal wave	
Different Thermoelasticity Theories	**Velocity (v_e)**	**Attenuation**	**Velocity (v_t)**	**Attenuation**
Green- Naghdi model-II	finite	No	finite	No
Green- Lindsay model (Aouadi (2005))	finite	Yes	finite	Yes
Green- Naghdi model-I	finite	Yes	infinite	Yes
Dual phase-lag model (Mukhopadhyay and kumar(2010))	finite	No	finite	Yes

Table 2.1(a). Comparative analysis of wave components of solution of temperature field under four models.

By using Boley's theorem (1962), we do study about the discontinuity of the physical field variables under the different models and find that the temperature function has no discontinuity in the case of GN-I model, however in the case of GN-II model and Green-Lindsay model, it has finite discontinuities at the wave-fronts $M_1(z-l)+t=0, N_1(z-l)+t=0$, and $\sqrt{A_1}(z-l)+t=0$, $\sqrt{A_1'}(z-l)+t=0$, respectively for GN-II model and Green-Lindsay model. The discontinuities found under Green-Lindsay model are similar to the same discussed in Aouadi (2005) and the discontinuity with finite jump in the temperature field is also seen in the case of dual phase lag model which are already reported by Mukhopadhyay and Kumar (2010).

Further, we have seen that the stress components represent six coupled waves in which three (modified elastic, modified thermal and shear waves) are originating at the upper surface of the plate while other three (modified elastic, modifies thermal and shear waves) are originating at the lower surface of the plate. For GN-II model and Green-Lindsay model, each and every stress components has the finite jump at the wave fronts which are given as $\eta_1(t)=M_1(z-l)+t=0, \eta_2(t)=-N_1(z+l)+t=0$, for GN-II model and $\eta_3(t)=\sqrt{A_1}(z-l)+t=0, \eta_4(t)=-\sqrt{A_1'}(z+l)+t=0$ for the Green-Lindsay model while the shear components are continuous

across the shear wave fronts $\frac{1}{\sqrt{\mu_1}}(z \pm l) + t = 0$ and shear waves propagate with the common non dimensional finite speed $\sqrt{\mu_1}$. We also note that the displacement component u along with its first order partial derivative with respect to z and t are continuous functions but its second derivative is discontinuous function with finite jump. The displacement component w is also continuous. Thermal parts of all the field variables are diffusive in the case of GN-I model. In the case of dual phase lag model as reported by Mukhopadhyay and Kumar (2010), the stress components have also been found to show finite jump discontinuities at the wave fronts.

2.5 Numerical results and discussion

In the previous section, we discussed the nature of solution of the field variables by obtaining the short-time approximated analytical solutions by using Boley's theorem (1962). Now, we make an attempt to carry out the numerical work to compute the numerical values of the physical fields under all four models: GN-I, GN-II model, dual phase-lag model and Green-Lindsay model to find out the different behavior of the field variables in the present context at the middle plane of the plate at any instant of time. The copper material has been considered for the purpose of numerical work and take the following data (given in Chandrasekharaiah and Srinath (1997)):
$\lambda = 7.76 \times 10^{10}\text{Nm}^{-2}$, $\mu = 3.38 \times 10^{10}\text{Nm}^{-2}$, $\alpha_t = 1.78 \times 10^{-5}\text{K}^{-1}$, $d = \frac{K}{\rho c_e} = 0.000113\text{m}^2\text{s}^{-1}$,
$c_e = 383.1\text{JKKg}^{-1}$, $\rho = 8954\text{Kgm}^{-3}$, $T_0 = 293\text{K}$, $\eta = \frac{1}{d}$, $\tau_1 = 0.02$, $\tau_2 = 0.03$, $\tau_q = 0.02$,
$\tau_T = 0.015$, $C_0 = 1$, $l = 1$, $K^* = \frac{c_v(\lambda+2\mu)}{4}$, $0 \leq r \leq 5$, $t = 0.13,\ 0.35,\ 0.69,\ 1.21$
The inversion of Laplace transform has been carried out by using the method given by Bellman *et al.* (1966) which is summarized in the Appendix-A2. Gauss-Laguerre quadrature integration method is used to invert the Hankel transforms. By using programming in MatLab, we carry out our computation to obtain the numerical values of physical field variables in the physical domain $(r; t)$ by inverting the solutions obtained in Laplace transform domain given by Eqs. (2.41-2.48). With the help of above non dimensional values and the expressions which are already discussed in the previous section, we have calculated the non-dimensional finite speeds in the context of all four models, namely GN-II model, GN-I model, Green-Lindsay model and dual phase-lag model. The velocity of waves under different models are tabulated in table 2.1(b). The speeds v_e's for elastic waves are obtained as 0.4835 and 0.9974 in the case of GN-II model

and Green-Lindsay model, respectively. However, in the case of GN-I model, it is computed to be exactly 1. The non-dimensional finite speeds v_t's for thermal waves are 1.1255 and 7.0729 in the case of GN-II model and Green-Lindsay model, respectively and in the case of GN-I model, it is diffusive in nature. From above, it is clear that the thermal wave reaches first the middle plane of the plate at non-dimensional times, 0.8885, 0.1414 under GN-II model and Green-Lindsay model, respectively. However, the elastic wave reaches there at non-dimensional times 2.0683 and 1.0026 in the contexts of GN-II model and Green-Lindsay model, respectively. On the contrary, in the case of GN-I model, the elastic wave reaches the middle plane of the plate at non dimensional time 1. We further note that in case of dual phase-lag model, the speeds of elastic, and thermal waves are 0.99942 and 8.6978, respectively. They reach the middle plane of the plate at non-dimensional times 1.009 and 0.1149 . This implies that the thermal waves reach the middle plane of the plate before the reaching the elastic waves there. From above, it is clear that the speed of elastic wave as well as thermal wave is smallest in the case of GN-II model whereas this speed is largest in the case of GN-I model. Hence, thermal wave reaches fast at the middle plane of the plate as compared to the elastic wave in the context of all four models. We find here that the wave speeds under Green-Lindsay model are exactly similar with the results as reported by Aouadi (2005) while the wave speeds under dual phase-lag model are found to be exactly similar with the results as reported by Mukhopadhyay and Kumar (2010).

	Elastic wave		Thermal wave	
Different Thermoelasticity Theories	Velocity (v_e)	Time to reach at middle plane of the plate	Velocity (v_t)	Time to reach at middle plane of the plate
Green- Naghdi model-II	0.4835	2.0683	1.1255	0.8885
Green- Lindsay model	0.9974	1.0026	7.0729	0.1414
Green- Naghdi model-I	1	1	infinite	-
Dual phase-lag model	0.99942	1.009	8.6978	0.1149

Table 2.1(b). Numerical values of elastic and thermal wave speeds under all four models.

All the physical field variables are represented graphically to show their variations for the different non-dimensional values of r and t. Figs. $(2.2-2.5)$ show the temperature distribution for different values of time, t verses the radial distance, r and Figs. $(2.6-2.9)$ represent the displacement distributions. The radial stress distributions are showed in Figs. $(2.10-2.13)$.

From Figures $(2.2-2.9)$, we see that at the initial time, the temperature and displacement fields corresponding to various models have a significant difference near the boundary but this difference decreases in cases of three models: GN-I model, Green-Lindsay model and dual phase-lag model with the increase of time while it is prominent in case of GN-II model. The values of these fields near the boundary increases with the increase of time only in the case of GN-II model. From Figures $(2.10-2.13)$, we also note that the stress fields have a significant difference at the initial time near the boundary for all models but this difference is more prominent for GN-II model. At the initial time, this value is minimum in the case of Green-Lindsay model, while it is maximum in the case of GN-II model. The value of this field decreases with increase of time in the case of GN-II model at the boundary while its value decreases in the case of other three models- GN-I model, dual phase-lag model and Green Lindsay model. The region of influence of all the physical fields in the context of all models increases with the increase of time.

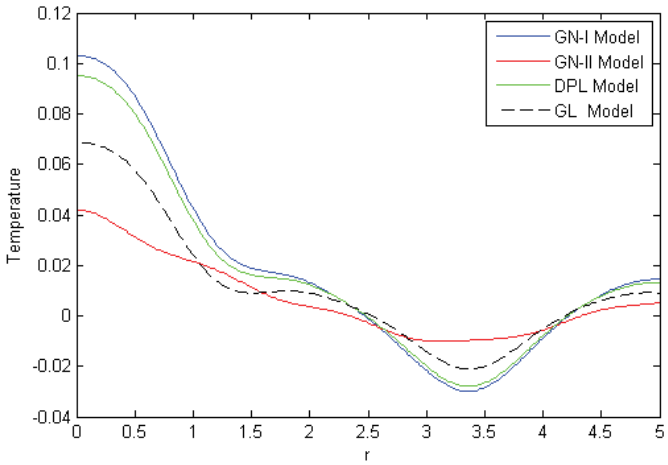

Fig. 2.2 Temperature distribution at t =*0.13*.

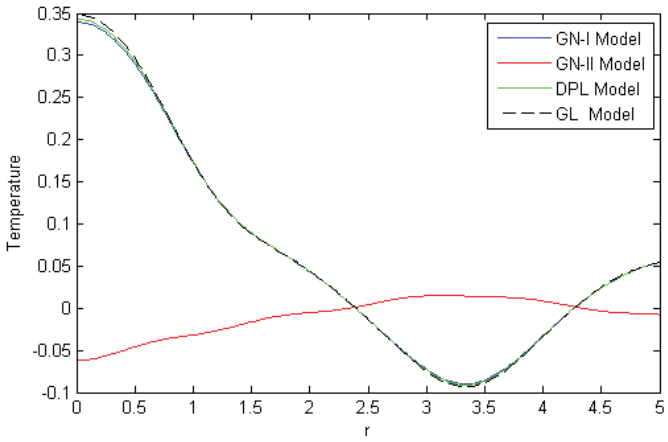

Fig. 2.3 Temperature distribution at $t = 0.35$.

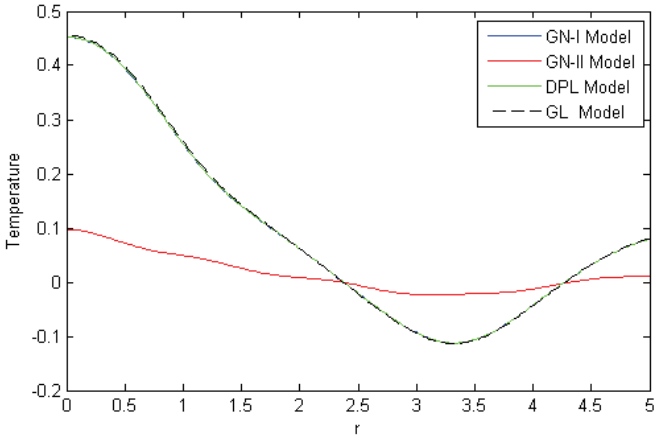

Fig. 2.4 Temperature distribution at $t = 0.69$.

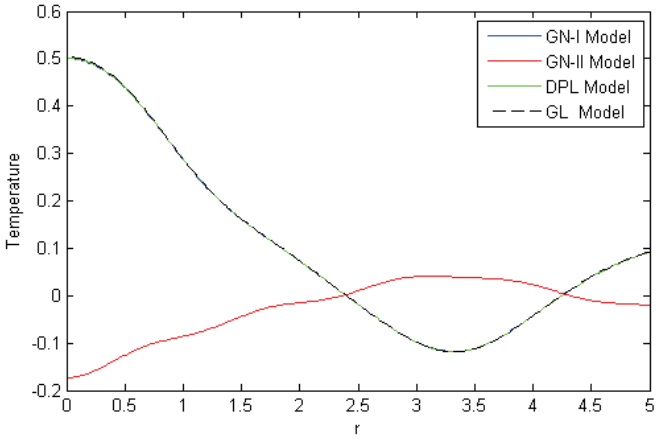

Fig. 2.5 Temperature distribution at $t = 1.21$.

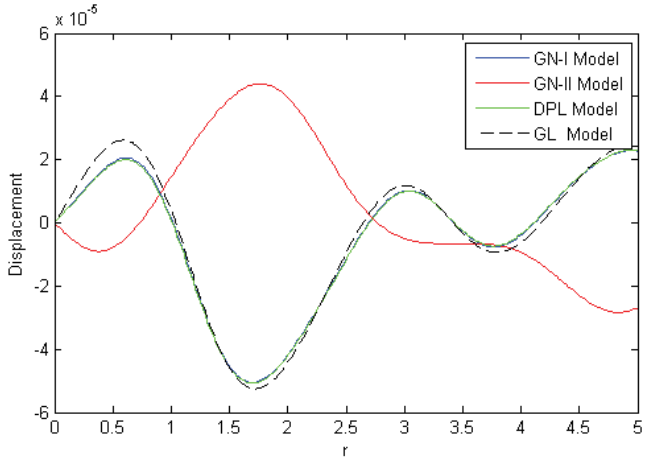

Fig. 2.6 Displacement distribution at $t = 0.13$.

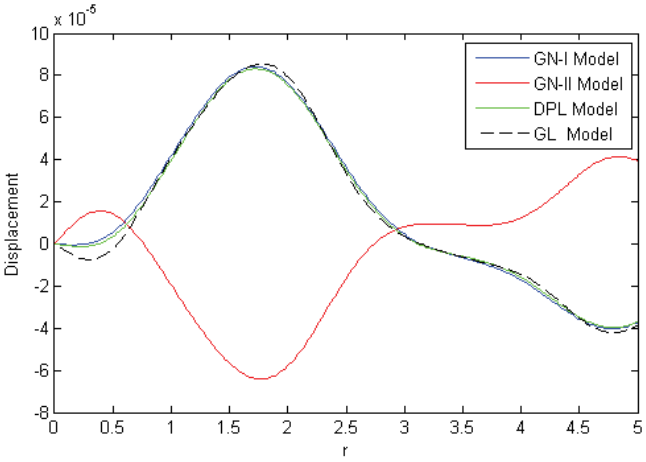

Fig. 2.7 Displacement distribution at $t = 0.35$.

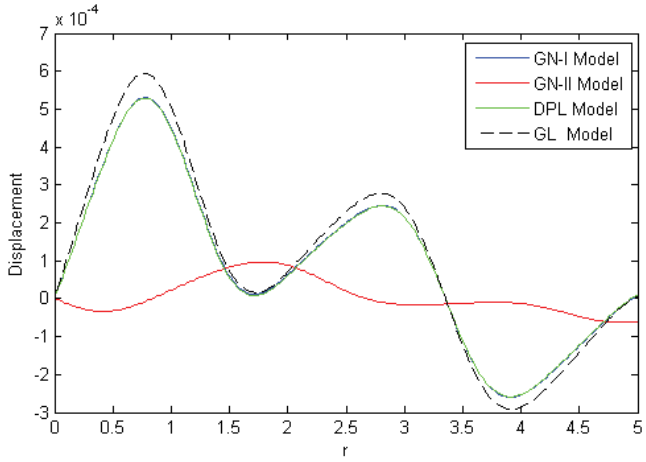

Fig. 2.8 Displacement distribution at $t = 0.69$.

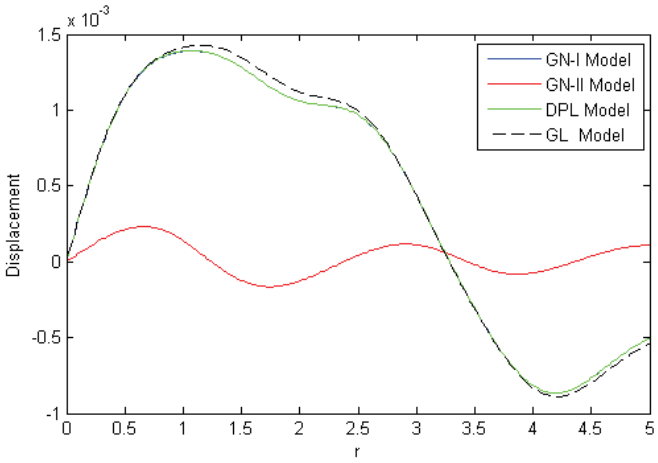

Fig. 2.9 Displacement distribution at t =1.21.

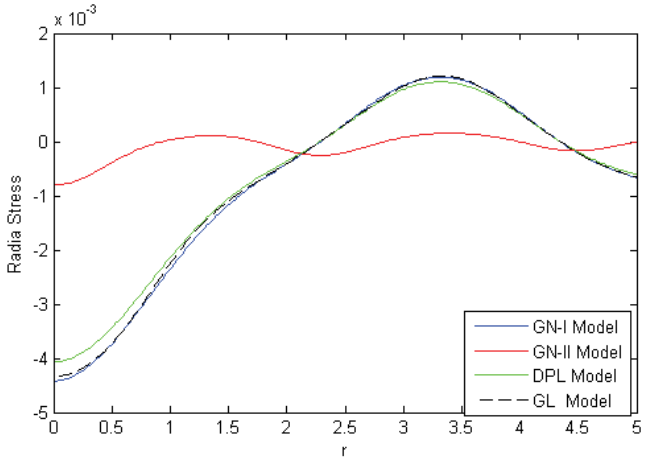

Fig. 2.10 Radial stress distribution at t =*0.*13.

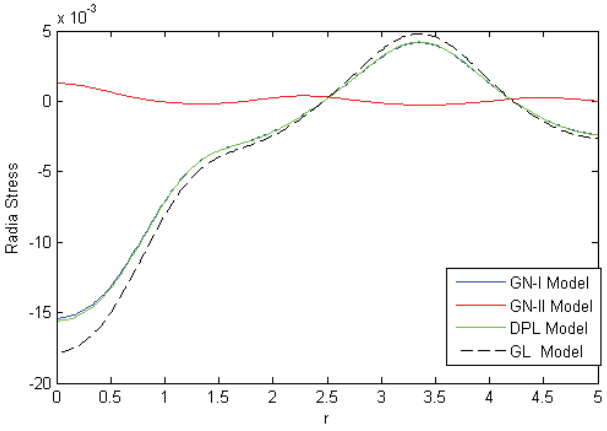

Fig. 2.11 Radial stress distribution at t =*0.*35.

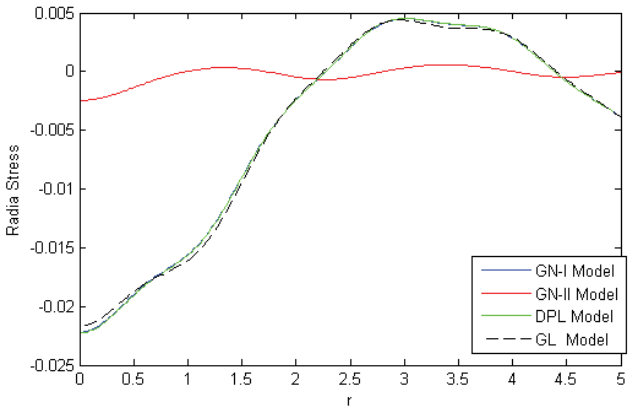

Fig. 2.12 Radial stress distribution at $t = 0.69$.

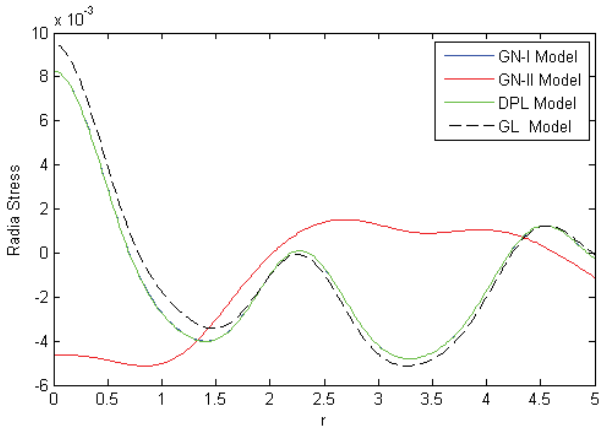

Fig. 2.13 Radial stress distribution at $t = 1.21$.

From above discussion, it is clear that the behavior of all the physical field variables predicted by GN-II model is completely different from the predictions by other three models: GN-I model, dual phase-lag model, Green-Lindsay model. This implies the disagreement of GN-II model to other three models. However, the prediction of GN-I model is nearly similar to the predictions by the other two models: dual phase-lag model and Green-Lindsay model.

2.6 Conclusions

In the present work, we aim to investigate recent heat conduction models: GN-I model, GN-II model, dual phase-lag model and Green-Lindsay model in generalized thermoelasticity theories in order to analyze the thermoelastic interactions inside an infinitely extended thick plate due to an axi-symmetric temperature distribution applied at the lower and upper surfaces of the

plate. We pay special attention to the model of thermoelasticity without energy dissipation and the following features of this model as compared to other heat conduction models have been investigated:

- The elastic as well as thermal waves propagate with finite speed under GN-II model. However, these waves propagate without any attenuation.
- Thermal waves reach first the middle plane of plate comparing to elastic waves in the case of all three models: GN-II model, Green-Lindsay model and dual phase-lag model.
- Thermal waves are not appeared only in the case of GN-I model due to the presence of damping term in the heat conduction equation.
- In the case of GN-I model, the temperature field shows a finite jump discontinuity at the elastic wave front while in the case of GN-I model, dual phase-lag model and Green-Lindsay model, the temperature field has a finite discontinuity at thermal and elastic wave fronts. The values of all the physical field variables increase with the increase of time and the region of influence is less in case of GN-II model.
- The behavior of all the physical fields in the case of GN-I model and Green-Lindsay model is almost similar in nature, although the Green-Lindsay model shows a small difference in results near the boundary and at lower time as compared to GN-I model and dual phase-lag model. However, the behavior of all the physical fields predicted by GN-II model is significantly different as compared to the behavior of all the field variables predicted by other three models at any time. Further, this difference increases with the increase of time for all the field variables.